MAGEL: AN ADVANCED PARTIALLY REUSABLE LAUNCH ARCHITECTURE CONCEPT

Stephen R. Steffes[*]
Dr. John R. Olds[†]
Space Systems Design Lab
School of Aerospace Engineering
Georgia Institute of Technology, Atlanta, GA 30332-0150

Abstract

Magel is an advanced partially reusable launch architecture which uses two large magnetically repelled superconducting rings as the first stage system and a liquid expendable rocket as the upper stage. This architecture is studied in an attempt to drastically reduce launch costs. The first stage is fully reusable and must be refueled before every launch. The only resources used are the upper stage rocket and the attitude control propellant. A full launch vehicle analysis is presented including an analysis of the system's feasibility and viability considering various technology tradeoffs. The baseline vehicle was found to be not feasible or viable even with infused technologies. For the baseline vehicle, the first stage ring is 6.6 km in diameter and 3.3 km high with a total dry weight of 15e6 lbs (6.8e6 kg). The cross section of the first stage ring is 2.2 m wide by 5.4 m high. Assuming a 56,900 lbs (25,800 kg) payload, 20 flights/year and a program length of 30 years, the total cost per pound to a 100 by 100 nmi 28.5° orbit is $35,500 FY2003/lbs.

Introduction

The high cost of access to space has greatly burdened advancements in space technology and exploration. Lowering this cost is an important step towards making space access more affordable. One way to drastically reduce launch costs is to use a new, advanced launch architecture. The use of magnetic fields to push a payload into space is one promising architecture type. Some designs that have explored this notion (Maglifter, BiFrost and StarTram) have produced optimistic results. Magel is another such architecture that utilizes magnetic fields and may hold the key for low cost access to space.

Magel has the same requirements as a Delta 4 Heavy (D4H). It is a cargo only vehicle capable of carrying 25,800 kg (56,900 lbs) to a 28.5°, 100 nmi by 100 nmi orbit around Earth. It launches from a ground facility located at least 17.5 km East of Kennedy Space Center (KSC) in the Atlantic Ocean.

Magel is an advanced partially reusable launch architecture which uses two large magnetically repelled superconducting (SC) rings as the first stage system and a liquid expendable rocket as the upper stage. Variations of this architecture will be studied in an attempt to drastically reduce launch costs compared to current expendables. A full disciplinary analysis of the vehicle is presented, as well as Monte Carlo simulations for the systems feasibility and viability.

Electrodynamics

Magel uses two physical dipoles for its first stage. The dipole moments are oriented in opposite directions so that they repel from one another. One dipole is stationary, on the ground, while the other is repelled upwards, towing the second stage rocket. To understand how this system works, basic electrodynamics must be discussed.

All magnetic fields are produced by electric currents. For a steady line current, the magnetic field is given by the Biot-Savart law:

$$\vec{B}(\vec{r}) = \frac{\mu_0}{4\pi} I \int \frac{d\vec{l} \times \hat{\mathfrak{R}}}{\mathfrak{R}^2}$$

where μ_0 is the permeability of free space, I is a steady line current, dl is a differential element of length along the current and $\mathfrak{R}$ is the vector from dl to r. Integration is along the current path in the direction of positive current flow.

When a particle with charge Q moves through a magnetic field, a force is applied to the particle according to the Lorentz force law:

$$\vec{F} = Q(\vec{v} \times \vec{B})$$

where F is the applied force, v is the velocity of the particle and B is the magnetic field that the charge is moving through. A magnetic field perpendicular to the current applies a force which is perpendicular to both the magnetic field vector and the current vector.

Consider two parallel steady line currents, I_1 and I_2. Each current produces a magnetic field which wraps around the current according to the Biot-Savart law. Each current is also in a magnetic field, which yields an applied force. If the two currents are in the same direction then the applied forces are such that the two currents are attracted towards each other. If the

---

[*] Graduate Research Assistant, School of Aerospace Engineering, Student member AIAA.
[†] Associate Professor, School of Aerospace Engineering, Senior member AIAA.

currents are in opposite directions then they repel.

Magel uses a system of two physical dipoles stacked on top of each other. A physical dipole is a circular loop of current which produces a magnetic field shown in Figure 1 (a). If two current loops of the same radius are stacked on top of each other with currents going in opposite directions (Figure 1 (b)) then the applied force on the upper loop due to the lower loop is as shown in Figure 1 (c). There is a net upward force on the loop. This force is the basis for the first stage of the Magel architecture.

Consider the case where two current loops are stacked on top of each other and the bottom loop is on the surface of the Earth. There is a gravitational force in the negative z direction pulling the top loop downwards. If the magnetic force on the loop balances out the gravitational force then the resulting system is unstable. If the center of the top loop shifts a small amount away from the z-axis then the net horizontal force on the upper loop is non-zero and there is a net torque. These are factors to consider when designing Magel.

Another issue to consider for this system is the case of a changing magnetic field due to the lower ring. Changing magnetic fields induce electric fields. These electric fields induce currents in conducting materials. This includes the conductor containing the current in the upper loop as well as any conductors in electronics, engine parts, second stage, etc. Materials exist that are known to soak up magnetic fields and can be used to protect sensitive components if the induced current is large.

The last topic to consider is superconductivity. There are a number of problems that come about by using conventional conducting materials (copper, iron or gold) to carry the current for the upper ring. These materials have small internal resistance which causes a loss of current and a build up of heat. They are also heavy materials compared to the alternative. SC materials have zero resistance which leads to zero loss of current and no heating. Generally, they are also lighter weight. The tradeoff is harder maintenance, elevated cost and higher complexity than conventional conductors. However, they are necessary to maintain the high currents needed for Magel.

Superconductors are materials that have zero electrical resistance and perfect diamagnetism when they are cooled below a certain temperature, called the critical temperature (T_c). Perfect diamagnetism means that the material does not allow an external magnetic field to penetrate into its interior. To counteract any applied field, a superconductor will induce its own magnetic field to exactly cancel it. As a result, a superconductor's T_c will lower with an increase in the
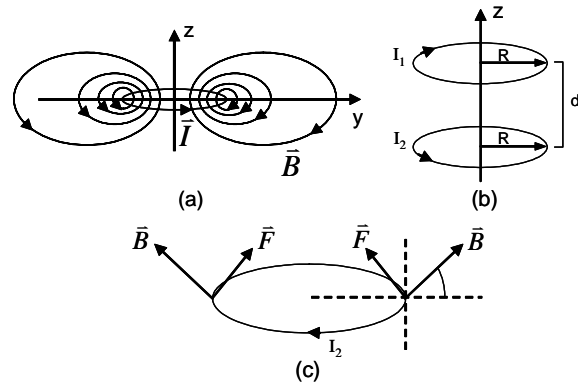

Figure 1: (a) Magnetic field of a physical dipole. (b) Stacked current loop configuration. (c) Force applied to upper current loop.
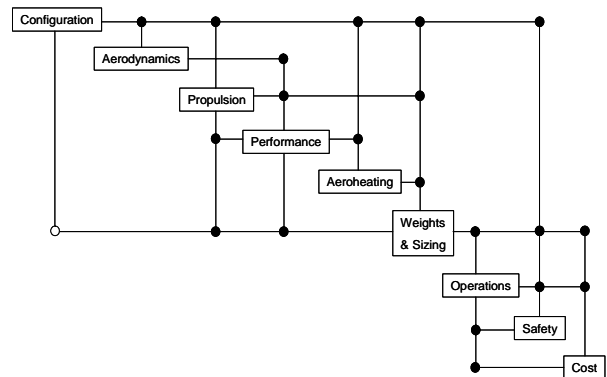

Figure 2: DSM used for Magel.

applied magnetic field, meaning too much magnetic field will cause the SC material to become non-superconducting.

Design Methodology

The design methodology used focuses on designing a launch system which is comparable to the D4H. The D4H was chosen because it currently has the largest payload capability of all expendables. To more closely compare the two systems, the second stage of Magel was based off of the second stage of the D4H.

Figure 2 shows the design structure matrix used to design Magel. There is a large convergence loop between the configuration and weights and sizing analyses. There is also a loop between operations and both cost and safety. The feedback link from weights and sizing to configuration is rather weak, so the configuration does not change often and the main convergence loop is between propulsion and weights and sizing.

Mission Scenario

The Magel architecture replaces the first stage of an expendable rocket with a reusable vehicle. The first stage of the system consists of a large (6.6 km diameter) ring that houses 7 SC tubes. These tubes carry enough current to propel the ring into the atmosphere by pushing against the magnetic field provided by the ground ring. The second stage of the system is an expendable rocket. During the ring's ascent, the second stage is towed behind the first stage, connected to the ring by cables.

At launch, the first stage and the attached second stage rest on top of the ground ring (Figure 3). When the two rings have been charged up to their initial current, the first stage is released. The first stage ascends upwards, towing the second, until the upward force on the ring vanishes. At this stage the vehicle is going 726 m/s vertically (Mach 2.44) at 20 km altitude. At that time the second stage is released from the cables and is ignited. This single stage rocket then ascends into a 100 nmi by 100 nmi 28.5° orbit. Shortly after the second stage is released (while the cables still have some horizontal motion towards the outside of the ring), the cables detach from the first stage, fall into the ocean and are later recovered. When the first stage starts to fall back down to Earth, it uses the magnetic force applied by the ground ring to slow its descent and make a soft landing back onto the ground ring. During the whole trajectory, the current of the ground site is controlled to yield the optimal performance.
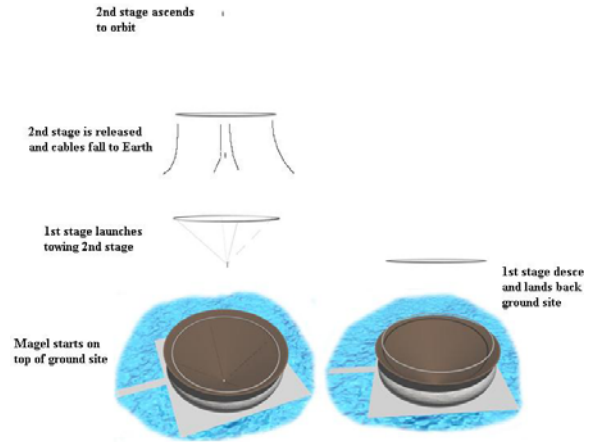
Disciplinary Analyses

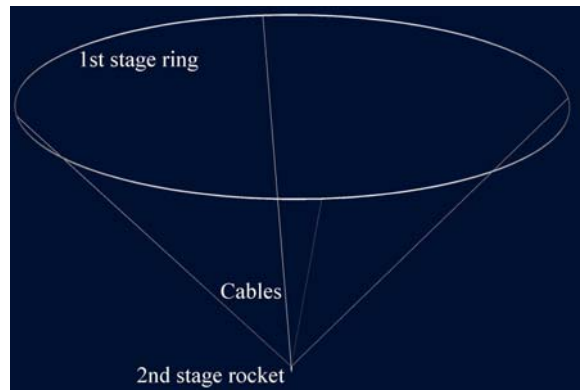Conceptual design of the vehicle used several disciplinary analyses to analyze the feasibility and viability of the system. They are presented here in order of execution within the design structure matrix.

Configuration

Configuration of the vehicle was determined using Pro/Engineer. Size estimates for each of the subsystems on the vehicle where obtained from the weights and sizing analysis. These values were used to draw a model of the system. This model was then used to determine available space and, more importantly, to provide a model for the aerodynamics analysis.

The baseline vehicle configuration is shown in Figure 4 and Figure 5. The second stage rocket is positioned on the axial line of the vehicle and is suspended from the first stage by 4 cables. These cables are angled at 45° with respect to the horizontal. The first stage ring is 6.6 km in diameter and the second stage hangs 3.3 km below the ring.

A closer view of the first stage shows more interesting details (Figure 6). The cross section of the ring is an airfoil shape with a height to width ratio of 2.5 (5.4m by 2.2m) (Figure 5). This allows enough
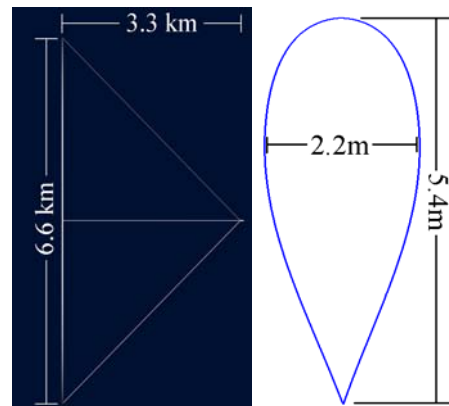

Figure 3: Magel mission profile.

Figure 4: CAD model of Magel (isometric view).

Figure 5: Side view (left) of Magel. Cross section of first stage ring (right).

volume to house 7 SC tubes, 4 attitude determination and control system (ADCS) engines and all of the ADCS propellant. There are 4 propellant tanks positioned around the ring, one for each ADCS engine.

Aerodynamics

Aerodynamics analysis was performed with Configuration Based Aerodynamics (CBAero) version

1.4.1. CBAero is a preliminary aerodynamics tool for predicting subsonic to hypersonic aerodynamic environments about an arbitrary vehicle configuration. For subsonic aerodynamics CBAero uses an unstructured, fast multi-pole panel formulation and for the supersonic and hypersonic regimes it uses a variety of independent panel type methods. This software is currently being developed by David J. Kinney at NASA Ames Research Center. The parts of the software that are still in development were not used in this analysis.

For the first stage trajectory, only the aerodynamics of the ring was considered. The components from the cables, second stage and engines were considered negligible. Analysis was done over the entire regime provided by the trajectory. Mach number (M) ranged from 0 to 3, dynamic pressure (q) ranged from 0 to 0.422 atm and angle of attack (α) was from 0 to 10°. The trajectory itself did not sway from an α other then 0°, but other α's were considered for completion.

CBAero provides lift and drag coefficients over the specified regime. For the first stage, Figure 7 shows C_{dt} vs M. This gives a peak C_{dt} of 0.76 at M=1.54. These results were accounted for in the performance analysis.

Propulsion

The design of the individual SC tubes was based on the StarTram design[1]. One tube consists of a structural support tube, an outer heat dispersing tube, the superconducting material and a flow of liquid helium. This design allows for good structural support and cooling of the SC material.

The main structure for each tube consists of a graphite epoxy honeycomb composite support tube. This supports the tube from collapsing in on itself due to the radially inwards magnetic pressure caused by the tube's own magnetic field. Tubes were designed to withstand 5 times their rated pressure in the worst case scenario to ensure an adequate safety margin.

Liquid Helium (LHe) flows through the support tube to cool the SC wires. NbTi has a T_c of 9.3 K, so the cooling fluid used must cool the SC wires to a temperature that is lower than this[2]. LHe is the best alternative in terms of cost, weight, boiling point and the fact that it is a noble gas. This will cool the wires to LHe's boiling point at 4.2 K.

The entire SC tube system was designed to have high safety margins and good structural support. 7 tubes carry the total current needed for the first stage (1.2e7 A). In the worst case scenario, 2 entire SC tubes are allowed to transition to their normal state and cease to carry current. If that happens, the current being carried by these tubes is transferred over to the other 5 tubes.

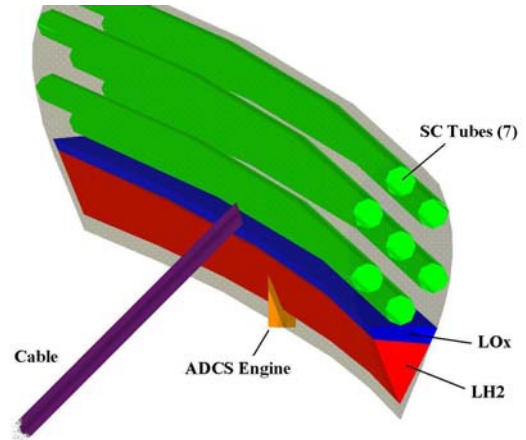The 7 SC tubes were configured into a "figure

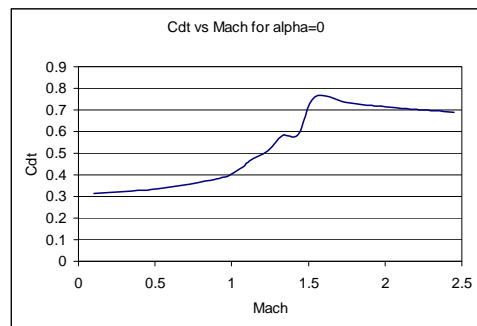**Figure 6: First stage ring breakdown, zoomed in.**

Figure 7: C_{dt} vs Mach for α=0 for the ring.

eight" geometry (Figure 8). This design provided good packaging inside the airfoil as well as structural support. Truss segments were positioned between several sets of SC tubes to support the structure and provide a counter force to the attractive force between each tube. Truss segments were made out of graphite epoxy with an operating compression strength of 7.5e8 N/m^2. The truss also provided support against the laterally inward force due to the ground magnetic field, which was at its maximum at the maximum altitude, as well as counteract the force coming from the tension in the cables connecting the second stage. Each truss segment was sized to withstand 5 times the maximum axial force to ensure a good safety margin. The truss is represented by the thick lines shown in Figure 8.

The propulsion analysis used electrodynamics and SC theory to size the current carrying system based on values from weights and sizing. Given M_{gross} and the maximum altitude, and assuming that the maximum current from the ground site is 200 times that of the first stage ring, it was possible to find the current needed in the first stage and maximum current of the ground site in order to cancel gravity at the maximum altitude. From the critical current density (J_c, the maximum allowable current per cross sectional area) and the critical magnetic field (B_c, the maximum allowable magnetic field in the SC material) of NbTi, it was then

possible to find the total cross sectional area of SC material needed, as well as find the minimum radius of each SC tube.

Analysis of the ADCS system was based on a rough estimate of the amount of propellant needed to correct a small change in the trajectory. Assuming the ADCS makes a trajectory correction to reposition the entire first stage so that it's directly over the center of the ground ring every time the first stage is off by 2 m, it takes 6 m/s of velocity change to reposition the vehicle and that a correction of this magnitude occurs 100 times over the entire first stage trajectory, the total delta V needed by the ADCS was 600 m/s. The thrust needed from each ADCS engine was sized to 150% of the thrust needed to counteract the maximum torque applied by the ground ring's magnetic field, which was 6.5e5 N.

Each ADCS engine is a sized Space Shuttle Main Engine (SSME). The amount of propellant needed for the ADCS was considerable (1.7e6 kg). In order to save mass, an efficient SSME was chosen over a pressure fed system which would add weight due to the pressurized gas needed. This assumes the technology that an SSME-type engine can be created such that it can start and stop quickly and repeatedly.

The second stage propulsion analysis was a simple model based on a modified rocket equation. The rocket was sized based on the total delta V needed to get to orbit. The delta V needed to make the flight with no losses is $V_{final} - V_{initial}$. The delta V loss from drag was estimated to be 0 m/s because the rocket starts its ascent where the atmosphere is very thin (0.15 kg/m^3 and 9.2 K-Pa). The delta V loss from gravity and from thrust vector control was based on the delta V loss from an average expendable and scaled by the distance from the initial altitude to orbit. There was also a delta V gain from Earth's rotation. A summary of these values is listed in Table 1.

Other masses were sized from existing vehicles. Inert mass and payload fairing mass were taken from the D4H[3]. Engine mass and I_{sp} were sized from an SSME based on the thrust required (120% of the total weight).

Performance

Performance calculations used a simple altitude step method to compute the trajectory of the first stage.
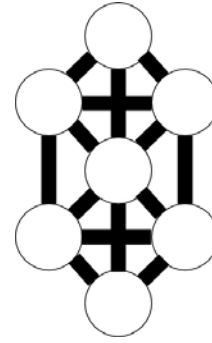

Figure 8: Truss and SC cable geometry.

Table 1: Delta V losses for the second stage.

Delta V Loss	Value	Units
Flight	7,068	m/s
Drag	0	m/s
Gravity	599	m/s
TVC	599	m/s
Rotating Earth	-396	m/s
Total	7,870	m/s

Values for the initial altitude, maximum acceleration (a_{max}=6 g's, based on D4H payload requirements), maximum q (q_{max}=42.6 KPa, from D4H payload fairing), gross mass (M_{gross}=1.10e7 kg) and the drag profile were provided. The maximum current of the ground station ($I_{g,max}$, where I_g is the current of the ground station) is the current needed to balance the gravitation force of the gross mass at an altitude of 20 km. Small steps in altitude (30 to 250 m) were taken until the maximum altitude was reached. At each step the trajectory conditions were calculated based on the previous step. The atmospheric model used simple equations from Glenn Research Center[4].

A final first stage altitude of 20 km was chosen to restrict the capabilities of the architecture. This ensures that the first stage does not escape from Earth. It provides a limit on the size of the vehicle. Also, it provides a staging point for the second stage that has little atmospheric density.

Each phase of the trajectory is limited by a_{max}, q_{max} or $I_{g,max}$. Initially the trajectory is limited by a_{max}, at the end of this phase q will rise to q_{max}. During the next phase, the vehicle accelerates slowly, keeping

Table 2: Conditions at key points in the first stage trajectory.

State	Time (s)	Alt (m)	Vel (m/s)	M	q (Pa)
Initial Condition, a=a_{max}, q<q_{max}	0.0	24	0	0.00	0
q=q_{max}, a<a_{max}	5.5	778	272	0.81	42,109
$I_{g,line}$=$I_{g,dipole}$, q=q_{max}, a<a_{max}	10.5	2,175	292	0.88	42,109
I_g=$I_{g,max}$, q<q_{max}, a<a_{max}	40.8	14,431	628	2.11	42,109
2nd Stage Ignition, q<q_{max}, a=0	48.8	20,000	726	2.44	23,453

q=q_{max}, until I_g rises to $I_{g,max}$. The vehicle then rises until a=0, at which point the second stage will ignite. There is also a point in the trajectory where the magnetic force from the ground station switches from using the calculation based on two circular line currents to the calculation based on two dipoles. At this point the current needed by a line current ($I_{g,line}$) is equal to a current needed by a dipole ($I_{g,dipole}$). This trajectory is the most efficient way to reach the maximum altitude with the given constraints (in terms of maximum final velocity). The conditions between each phase in the trajectory are listed in Table 2.

The equations used to calculate the magnetic force are based on the force between two circular line currents and between two dipoles, as discussed earlier. The actual equations used are the same as those discussed, but with an added geometric imperfection factor. This constant multiplies the original equations to create more conservative calculations. For this geometry, the value used for this constant was 0.9 . The imperfection was used because these equations are only approximations. The exact expressions for the force equations are much more complicated.

The conditions throughout the first stage trajectory are shown in Figure 9. There are abrupt changes in the charts due to transitions between each phase of the trajectory, as expected. The largest concern here is the discontinuity in the magnetic field at the first stage due to the ground site at the end of the first phase. This is due to the large change in acceleration at this point. To control this change, the current in the ground facility must quickly change from a value of 1.03e7 A to 2.65e6 A in less than one second. Realistically, changes in current at this rate are not feasible with current technology. One alternative would be to gradually change the current over this point. The

analysis assumed that the ground site has complete control over the current in the ground ring to simplify the trajectory.

The maximum rate of change in magnetic field at the first stage is small (~6.1e-4 T/s, not including the discontinuity). This is a small rate (the Earth's magnetic field is 4.5e-5 T at the surface), although their still may be some problems with induced electric currents in subsystems. The amount of material needed to protect sensitive components was assumed to be negligible when compared to the mass of the first stage. The amount of current that is gained from this change in magnetic field was also assumed to be negligible.

Aeroheating and Thermal

Miniver was used for the aeroheating analysis. This code predicts aeroheating boundary conditions for a given cross section, trajectory and ambient conditions. It was developed by NASA Langley Research Center in the early 90's. Analysis was only done for the first stage ring because the contribution of thermal protection system mass due to any other part of the vehicle is negligible compared to the mass of the ring.

Results from Miniver consisted of peak temperature values on the airfoil. The peak temperature attained was 451.7 K at the top of the cross section. A conservative estimate for the melting point of aluminum (the material on the skin of the ring) is 533 K. Therefore, there is no need for any thermal protection system (TPS) on the ring skin.

TPS for the rest of Magel was neglected. Realistically, there may be impinging sock waves on the cables. There may even be a shock cone that intersects with the second stage. Heating effects due to these cases were assumed to be small enough such that the problem could be solved by addeingTPS to the
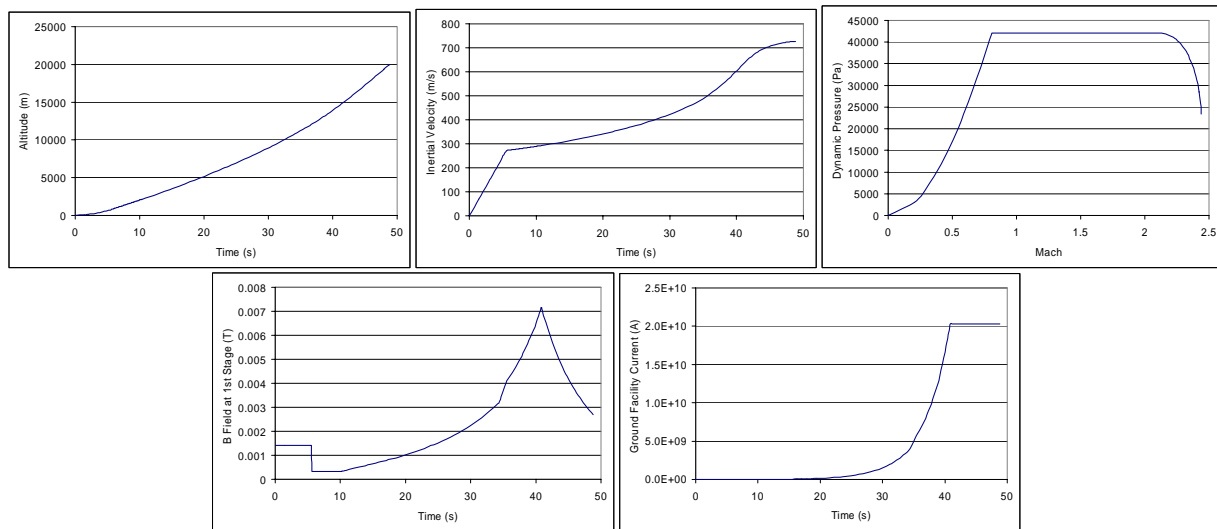

Figure 9: Conditions for the first stage trajectory.

effected areas. The weight of this TPS was assumed to be much smaller than that of the entire vehicle, and thus was neglected.

Weights and Sizing

Magel was sized based on existing components, estimations from StarTram and reusable launch vehicle (RLV) mass estimating relationships. This analysis was spreadsheet based, using inputs from the configuration, propulsion, performance and aeroheating analyses. It produced values for subsystems masses, total mass and vehicle dimensions (Table 3, Figure 10). The dry mass of the vehicle was 6.75e6 kg (1.49e7 lbs) and gross mass was 1.10e7 kg (2.41e7 lbs).

There were four main components for the first stage body: the ring fairing, ring truss, SC material and SC tubes. The amount of SC material needed was sized from the J_c and the radius of the first stage ring. The SC tubes were sized from the ring radius and the amount of magnetic pressure imposed and the radius of each tube was sized from the StarTram tube design. Mass for the ring fairing used a mass estimating relationship for RLV wing fairing weight[5]. Each strut composing the truss was sized based on the maximum axial force it needs to support as well as the ring radius.

The cooling system mass was sized from the SC tube size. This system consists solely of the LHe flowing inside each of the SC tubes. Mass of the LHe assumed that there was at most a 15 cm thick flow on the inside of each tube. Masses for other parts of the cooling system were assumed to be negligible compared to the mass of LHe.

Cables connecting the second stage were sized based on the maximum tension in each cable and are made from oriented polyethylene. Each cable runs from the first stage ring down to the second stage at a 45° angle. A 400% safety margin on the operational tensile strength was used.

The radius of the first stage ring as well as the radius of each SC tube was an independent variable for the mass analysis. The vehicle can be closed within a range of values for these radii. Outside these ranges, the mass of the vehicle blows up. These variables were optimized such that the life cycle cost (LCC) of the vehicle was minimized.

Operations

The operations analysis used Architecture Assessment Tool-enhanced (AATe), originally developed by NASA KSC. AATe is a spreadsheet based program that allows for quick estimations for fixed and variable operations costs as well as the vehicle turn around time and available flight rate.

Magel's operation settings were specified for AATe. Some assumptions include: Magel is a highly automated system and uses a dedicated turnaround and

Table 3: Scale of Magel baseline.

Name	Value	Units
Diameter First Stage	6,556	m
Airfoil Width	2.2	m
Airfoil Height	5.4	m
Total Airfoil Volume	160,000	m3
Diameter SC Tube	0.83	m
Cable Length	4,636	m
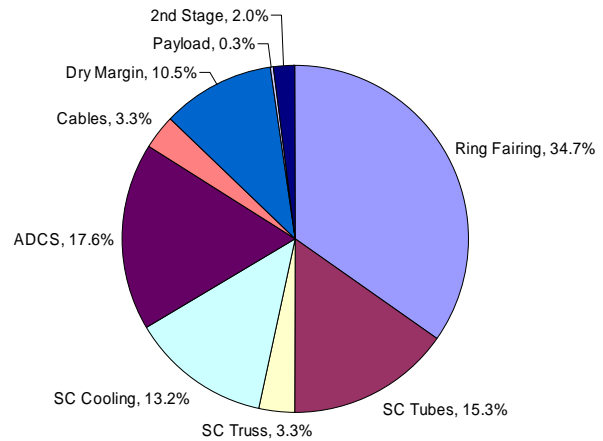
Figure 10: Weight breakdown for Magel baseline.

Table 4: Baseline operations metrics.

Name	Value	Units
Turn Around Time	14.3	Days
Available Flight Rate	25.5	Flts/Yr
Fixed Ops.	27,300	FY2003 M/Yr
Variable Ops.	9.70	FY2003 M/Flt
Facilities	3,010	FY2003 M/Site
Variable Labor	7.30	FY2003 M/Flt
Variable LRU	2.39	FY2003 M/Flt
Fixed Labor cost	104	FY2003 M/Yr
Fixed LRU	30.8	FY2003 M/Yr

assembly facility, it does not require the use of toxic or polluting materials, it is completely fault tolerance to support flight safety, but accepts loss of mission, Magel requires no on-board stored gases and all systems have non-intrusive and non-mechanically active sensors.

Baseline operations outputs from AATe are given in Table 4. Fixed operations cost was largely due to the size of the vehicle. Therefore, a large value for the fixed operations cost was reasonable compared to the overall size of Magel. The facilities cost was much smaller than expected due to the fact that AATe does not take into account launch assist systems. This cost was increased in the vehicle cost analysis to more accurately account for the complex ground system. Finally, AATe does not take into account that fact that

the second stage was expendable. The cost of the second stage was added to the variable operations cost in the cost analysis.

Safety and Reliability

Safety and Reliability analysis used GT-Safety II v1.6. This is a spreadsheet based code that works by multiplying various failure rates together. Values from the configuration, operations and weights and sizing were used to obtain the vehicle's reliability. Separate analyses were done for each stage of the vehicle.

For the first stage, all of the safety adjustment factors in GT-Safety were set to best describe the first stage of Magel. Magel was assumed to be 4 times safer than Space Shuttle in terms of abort options/windows, internal vehicle health monitoring, flight system redundancy, safety margins and ground handling complexity. Landing area flexibility was assumed to be 10 times less safe than Space Shuttle because Magel can only land directly on the ground site. The single engine shutdown rate was sized with the ring radius (7 SC rings were considered to be the first stage main engines). Propellant type versus TNT equivalent was sized with the total ADCS propellant. Lastly, vehicle subsystem failure rates were set to 10% of those for an average expendable.

For the second stage, the safety adjustment factors were set to describe a future expendable. The second stage was assumed to be 10 times safer than Space Shuttle in terms of vehicle health monitoring, ground handling complexity, the propellant loading process, and staging and flying over a population. It was also assumed to be mildly safer than Space Shuttle in terms of safety factors. The single engine shutdown rate was assumed to be the average for a rocket engine at 1 in 6,000. As for the first stage, the values for the vehicle subsystem failure rates were set to 10% of those for an average expendable.

According to GT-Safety, the baseline vehicle is very safe with these assumptions. The mean flights between failures (MFBF) for a loss of mission is 1 in 2,248 flights and for a loss of vehicle it is 1 in 5,076 flights. This is roughly 12 times the reliability of Space Shuttle. Note that a loss of the second stage vehicle was considered as a loss of mission for the whole vehicle.

One safety concern that was not handled by GT-Safety is the effect of the magnetic field of the ground current on the environment. Humans can with stand being in a magnetic field of 1.5 mT or in a changing magnetic field of 0.03 T/s without harm[6,7]. The minimum lateral distance away from the ground site where these conditions are satisfied is 17.5 km. Therefore, if the ground site is to be placed near KSC, it must be at least 17.5 km out in the ocean.

Cost and Economics

Cost estimation of Magel used the NASA-Air Force Cost Model (NAFCOM). This uses a historical database to estimate cost based on subsystem weights. Airframe and propulsion costs are estimated separately. NAFCOM was used to estimate the design, development, testing and evaluation (DDT&E) and theoretical first unit (TFU) cost for both the Magel vehicle and ground site.

For the vehicle estimation, component weights for each subsystem on each stage were input. Next, complexity factors for each cost component were determined. The first stage was said to be built in segments that are 16 m long (the length of a railroad car). Each of these segments are very similar; only difference being the four segments with ADCS engine and cable connections, the eight segments with end caps on the ADCS propellant tanks and some segments have ADCS propellant tanks in them and some do not. Therefore, all segments were estimated to be the same cost and a learning curve was used for each segment, assumed to be 85%. Also, the complexity factors for integration, assembly and checkout for both the airframe and the first stage propulsion were scaled from the number of segments.

A similar approach was used for the ground site cost estimation. The ground ring was considered to be much less complex than the launch vehicle because it is only composed of SC rings and it does not have to be flight ready. This assumption lowered complexity

Table 5: Economic results for Magel baseline.

DDT&E (Launch Vehicle and Facilities)	112	B$ FY 2003
TFU (Launch Vehicle Only)	29.7	B$ FY 2003
Facilities Cost (Includes Facilities Operations Cost)	48.0	B$ FY 2003/Site
Fixed Cost	27.5	B$ FY 2003/Yr
Variable Cost (Includes 2nd Stage Cost)	64.4	M$ FY 2003/Flt
Cost Margin (15%)	182	B$ FY 2003

| LCC | 1,210 | B$ FY 2003 |
| Price per lbs | 35,500 | $ FY 2003/lbs |

factors across the board and is responsible for its relatively low cost compared to its weight. The total facilities cost per site used was the sum of the cost from NAFCOM and AATe.

The economic analysis used was a spreadsheet based tool created solely for Magel. It simply sums the LCC of the vehicle assuming values for the engine life, vehicle life, program length and flight rate. It also assumes that the market does not change over the life of the vehicle, there is no profit and there is zero cost of money. This implies that the cost of the vehicle (TFU and DDT&E) is paid for upfront. Economic results for the baseline vehicle are given in Table 5.

Baseline Conclusions

The Magel baseline yields a price per pound that is not competitive with current expendables. The D4H costs a conservative $3000/lbs for a 100 nmi by 100 nmi orbit. Magel's cost is roughly 12 times that; not an outrageous amount, but enough not be competitive. However, these cost results involve some economic uncertainty. In order to get a better estimate of Magel's viability, a Monte Carlo simulation (MCS) was done, which will be explained later.

There are still several problems with the Magel architecture. There are impinging shockwaves on the cables as well as a possible impinging Mach cone on the second stage. The two stacked current ring geometry is unstable, which leads to the large ADCS system mass. Corrections due to high winds or the Coriolis Effect were not considered and may also make large contributions to the ADCS. Structural modes in the first stage ring and cables may prove to make the airframe unstable. There are induced currents in anything conductive on the vehicle due to the changing magnetic field of the ground ring. Not to mention the problems from the shear size of the vehicle.

Finally, there were several issues with the tools used for this design. NAFCOM, AATe and GT-Safety were created for normal RLVs, like Space Shuttle. Most likely, Magel is outside the acceptable limits of these tools. Therefore, other, more general tools are needed for better estimations. Still, these tools provide rough estimates for the vehicle and are a good first step.

ROSETTA Model

After the baseline vehicle was designed, a Reduced-Order Simulation for Evaluating Technologies and Transportation Architectures (ROSETTA) model was built. This is a spreadsheet based tool that fully integrates all components of the design into a simple tool to quickly estimate the effects of small changes in variables. It is necessary, when running a large number of cases for the input variables, to considerably reduce the computation time for each point in the design space.

Economic Monte Carlo Simulation

The baseline cost results contain various economic uncertainties. In order to get a better estimate of Magel's viability, an MCS was done. Economic variables are considered to be noise variables so triangular probability density functions were used over their ranges. These variables as well as their ranges are listed in Table 6.

After running the MCS, cumulative distribution functions were created for each of the economic metrics. Values for these metrics at the 50% confidence mark were considered to be the final results (Table 7). This gives a price per pound to orbit of $38,900 FY 2003/lbs; which is roughly 13 times that of a D4H. With these economic assumptions, the baseline Magel architecture is most likely not viable (especially since the 0% confidence of price per pound is $18,700 FY 2003/lbs).

Technology Infusion

To help improve the feasibility and viability of Magel, several technologies were considered. Since the SC tube mass is the main driver for the design, the main focus of the technology infusion was on different types of SC materials. These technologies were infused into the baseline and the resulting designs were compared.

Technology Identification

Three different types of SC materials were considered as well as technology impacts on magnetic field geometry and subsystem masses. SC materials considered include NbTi, Nb_3Sn and $(Bi,Pb)_2Sr_2Ca_2Cu_3O_x$ (BSCCO). For other technologies, general improvement in the geometric

Table 6: Economic variables and their ranges used for the economic MCS.

Variable	Min	Nominal	Max	Units
Engine Life	100	500	1,000	Flts
Vehicle Life	100	1,000	2,000	Flts
Program Length	1	30	50	Yrs
Learning Curve Rate	0.75	0.85	1	
Flight Rate	0	20	40	Flts/Yr
TFU Complexity Factor	0.5	1	1.5	
DDTE Complexity Factor	0.5	1	1.5	

American Institute of Aeronautics and Astronautics

imperfection factor, ADCS mass, airfoil fairing mass, SC truss mass and SC support tube mass were considered.

NbTi is the most common SC material currently in use and was used as in the baseline design. Typical values for density, J_c and B_c are 6,530 kg/m^3, 5e9 A/m^2 and 12.2 T respectively[8,1,2]. Large quantities are used in the competitive MRI magnet business and have brought the cost down considerably. The current estimate is around $1 FY2001/k-Am[9].

Nb_3Sn is another common SC material currently in use. Typical values for density and B_c are 8,036 kg/m^3 and 19.0 T[8,2]. A promising value for J_c of 6e9 A/m^2 has also been reported[10]. Currently, only small quantities of Nb_3Sn are being produced (2.5 tons/year) for an expensive $4.6 FY 2001/k-Am. If the demand for this material reaches 250 tons/year, this price could be brought down to $1.5 FY 2001/k-Am. Magel would create this demand, therefore, the lesser cost was assumed.

The leading high temperature superconductor is BSCCO. Currently, BSCCO is only available in powder form. Tubes of the material have been demonstrated to have peak values for J_c of 2e9 A/m^2, but only locally[11]. Typical values for density and B_c are 4,010 kg/m^3 and 465.5 T[8,2,11]. The current cost of BSCCO is $1,000 FY2001/k-Am[12]. With decreases in costs and new manufacturing techniques, the cost of BSCCO is predicted to decrease considerably to $21 FY 2001/k-Am. This smaller cost was assumed for the following analyses.

Improvements in other subsystems are not related to specific technologies, but represent general improvements that can be expected. Mass improvements in the airfoil fairing, SC truss and SC support tubes were based on improvements in materials. For the ADCS mass, once technology improvement could be to include all of the ADCS functionality in the ground ring or have some other ground based ADCS system. Therefore, a lower bound of 0 on the ADCS mass could be expected. Finally, improvements for the geometric imperfection factor were based on different ground ring geometries that could be considered.

Technology Monte Carlo Simulation

In order to evaluate the effects of infusing each technology, several MCSs were performed. The effects of infusing each of the SC materials were well understood. Instead of including each of these materials in a single MCS, three separate MCSs were run (one for each SC material). For example, one MCS consisted of infusing Nb_3Sn and running the MCS over the other five technologies. Technology impact factors used for the SC materials and the ranges used for the other technologies are listed in Table 8 and Table 9. The values for the SC materials were derived from the

Table 7: Economic metrics at 50% probability.

Metric	Value at 50% Confidence	Units
DDT&E	$113	B$ FY 2003
TFU	$30.2	B$ FY 2003
Facilities Cost	$48.8	B$ FY 2003/Site
LCC	$1,130	B$ FY 2003
Price per lbs	$38,900	$ FY 2003/lbs

Table 8: Technology impacts for SC material.

	NbTi	Nb3Sn	BSCCO
Density SC Material	1	1.23	0.614
Jc	1	1.20	0.4
Bc	1	1.56	38.1
Cost SC Material	1	1.5	21

Table 9: Ranges for general technology impacts considered.

Technologies	Min	Nominal	Max
Geometric Imperfection Factor	1	1	1.1
Mass ADCS	0	0.5	1
Mass Airfoil Fairing	0.8	0.9	1
Mass SC Truss	0.8	0.9	1
Mass SC Support Tube	0.8	0.9	1

values previously stated. The ranges for the other technologies were based on general improvements that could be expected.

After infusing each of the SC materials, the radius of the first stage ring and the radius of each SC tube was again optimized to minimize LCC. Gross mass for Nb_3Sn was 1.10e7 kg and for BSCCO was 1.23e7 kg. Cost per pound to orbit for Nb_3Sn was $35,700 FY 2003/lbs and was $41,300 FY 2003/lbs for BSCCO. Both of these technologies showed an increase in gross mass and cost compared to the baseline.

MCSs were then run on these three vehicles. The 50% confidence values are listed in Table 10 for each of the metrics. Assuming 20 flights per year for 30 years, these lead to costs per pound of $35,400 FY 2003/lbs, $35,700 FY 2003/lbs and $41,000 FY 2003/lbs for NbTi, Nb_3Sn and BSCCO respectively. NbTi is the most economically viable and feasible out of the three SC materials investigated. The other two materials have different tradeoffs but each one yields a final design that is more expensive than NbTi.

Technology Sensitivities

It is also useful to look at the effect that the individual technologies have on the vehicle. This will suggest which technologies to put development funds into. Each technology was individually applied to the

Table 10: 50% confidence levels for the three MCSs.

Metric	NbTi	Nb3Sn	BSCCO	Units
DDT&E	$98.4	$101	$177	B FY 2003
TFU	$25.4	$27.3	$103	B FY 2003
Facilities Cost	$43.6	$43.9	$50.0	B FY 2003/Site
Fixed Operations Cost	$28.3	$28.3	$28.3	B FY 2003/Yr
Variable Operations Cost	$62.6	$62.6	$62.8	M FY 2003/Flt
LCC	$1,210	$1,220	$1,400	B FY 2003
Gross Mass	8,850	8,890	9,960	MT
Loss of Mission Reliability	2250	2250	2242	MFBF

baseline while the vehicle metrics were recorded. The new values for each metric were compared to the baseline values to find the amount that each changed by applying the technologies. The sensitivities for the vehicle's gross mass and LCC are shown in Figure 11.

Both SC materials induce a increase in both gross mass and LCC. This is mostly due to the fact that these materials increase the gross mass and that the propulsion subsystem is the driving component of the vehicle. On the other hand, all of the other technologies show a decrease in gross mass and LCC. This is because all of these technologies either decrease subsystem masses or decrease the current needed.
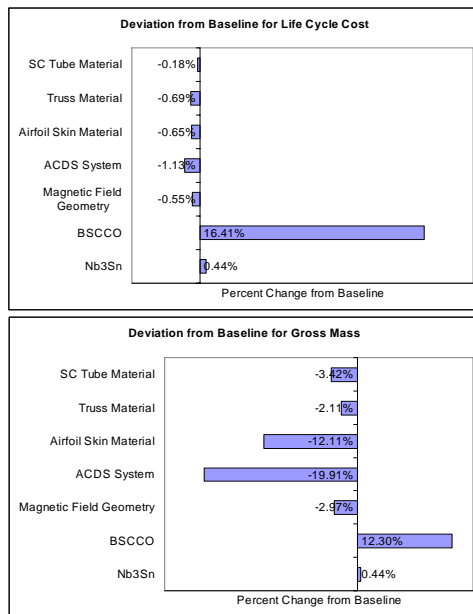

Figure 11: LCC and gross mass sensitivities.

<u>Conclusion</u>

The Magel baseline was not viable and did not seem feasible. The vehicle cost too much and was too large. By infusing technologies the vehicle became more and more viable and feasible. However, with the technologies considered, the vehicle was still not good enough. The largest problem is the underlying physics of the architecture. The magnetic field from the ground station decreases too quickly with altitude and the geometry is unstable. The greatest hope for this vehicle is to find a SC material or a magnetic field geometry that will reduce the gross mass and cost considerably.

[1] Powell, J. R., Maise, G., Paniagua, J., "StarTram: A New Approach for Low-Cost Earth-to-Orbit Transport," IEEE, 0-7803-6599, February, 2001.

[2] Poole, C. P., Farach, H. A., Richard, J. C., "Superconductivity," Academic Press Inc., 1995.

[3] Isakowitz, S. J., Hopkins, J. P., Hopkins, J. B., "International Reference Guide to Space Launch Systems," 3rd ed., AIAA, 1999.

[4] Benson, T., "Earth Atmosphere Model," June 4, 2002, http://www.grc.nasa.gov/WWW/K-12/airplane/atmos.html.

[5] Rohrschneider, R., "Development of a Mass Estimating Relationship Database for Launch Vehicle Conceptual Design," AE8900 Special Project, Georgia Institute of Technology, April 26, 2002.

[6] Mannix, R., "Static Magnetic Field (0 Hz) Safety," University of California, EH & S.

[7] "Magnetic Fields: Health and Safety Guide," World Health Organization, IPCS International Programme on Chemical Safety, Health and Safety Guide No. 27, 1989.

[8] "Solids: Properties of Solid Materials," V3.5, CryoSoft, March 2002.

[9] R. M. Scanlan, "Conductor Cost/Performance Status Report for Snowmass 2001," February 15, 2001.

[10] Hart, P. B., et. al., "Microstructure, Impurity Content and Critical Current Density in Nb3Sn," Journal of Applied Physics, April 1969.

[11] Larbalestier, D. C., Hellstrom, E. E., "Applied Superconductivity Center: BSCCO," U of Wisconsin-Madison, http://www.asc.wisc.edu/bscco/bscco.htm, March 1, 2002.

[12] Grant, P. M., Sheahen, T. P., "Cost Projections for High Temperature Superconductors," Applied Superconductivity Conference, September 1998.